Journal of Medicinal Chemistry

Drug Annotation

Discovery of N-(3-carbamoyl-5,5,7,7-tetramethyl-5,7-dihydro-4H-thieno[2,3-c]pyran-2-yl)-lH-pyrazole-5-carboxamide (GLPG1837), a Novel Potentiator which can open Class III Mutant Cystic Fibrosis Transmembrane Conductance Regulator (CFTR) Channels to a high extent.

Steven Emiel Van der Plas, Hans Kelgtermans, Tom De Munck, Sébastien Laurent Xavier Martina, Sébastien Dropsit, Evelyne Quinton, Ann De Blieck, Caroline Joannesse, Linda Tomaskovic, Mia Jans, Thierry Christophe, Ellen Van der Aar, Monica Borgonovi, Luc Nelles, Maarten Gees, Pieter FW Stouten, Jan Van Der Schueren, Oscar Mammoliti, Katja Conrath, and Martin J. Andrews

J. Med. Chem., **Just Accepted Manuscript** • DOI: 10.1021/acs.jmedchem.7b01288 • Publication Date (Web): 17 Nov 2017

Just Accepted

ACS Publications

Journal of Medicinal Chemistry is published by the American Chemical Society. 1155 Sixteenth Street N.W., Washington, DC 20036

Discovery of N-(3-carbamoyl-5,5,7,7-tetramethyl-5,7-dihydro-4H-thieno[2,3-c]pyran-2-yl)-lH-pyrazole-5-carboxamide (GLPG1837), a Novel Potentiator which can open Class III Mutant Cystic Fibrosis Transmembrane Conductance Regulator (CFTR) Channels to a high extent.

Steven E. Van der Plas†, Hans Kelgtermans†, Tom De Munck†, Sébastien L. X. Martina†, Sébastien Dropsit†, Evelyne Quinton†, Ann De Blieck†§, Caroline Joannesse†, Linda Tomaskovic‖, Mia Jans†, Thierry Christophe†, Ellen van der Aar†, Monica Borgonovi‡, Luc Nelles †, Maarten Gees†, Pieter Stouten†, Jan Van Der Schueren†, Oscar Mammoliti†, Katja Conrath†*, Martin Andrews†*

†Galapagos NV, Generaal De Wittelaan L11 A3, 2800 Mechelen, Belgium

‡Galapagos SASU, 102 avenue Gaston Roussel, 93230 Romainville, France

‖Fidelta Ltd., Prilaz baruna Filipovića 29, Zagreb, HR-10000, Croatia

KEYWORDS

Cystic fibrosis, CFTR, potentiator

ABSTRACT

Cystic fibrosis (CF) is caused by mutations in the gene for the cystic fibrosis transmembrane conductance regulator (CFTR). With the discovery of Ivacaftor and Orkambi, it has been shown that CFTR function can be partially restored by administering one or more small molecules. These molecules aim at either enhancing the amount of CFTR on the cell surface (correctors) or at improving the gating function of the CFTR channel (potentiators). Here we describe the discovery of a novel potentiator GLPG1837 which shows enhanced efficacy on CFTR mutants harboring Class III mutations compared to Ivacaftor, the first marketed potentiator. The optimization of potency, efficacy and pharmacokinetic profile will be described.

INTRODUCTION

Cystic fibrosis (CF) is the most common life-threatening autosomal recessive disorder in Caucasian populations, affecting approximately 70,000 patients worldwide.[1] It is caused by mutations of the gene for the cystic fibrosis transmembrane conductance regulator (CFTR) protein.[2] The ion channel CFTR is involved in the gating of chloride ions across epithelial cell membranes in various tissues including the lung, pancreas, intestine, reproductive tract and sweat duct. Although CF is a systemic disease, the most severe effects come from the reduced chloride secretion in the airways. Subsequent lung surface dehydration leads to the buildup of a thick mucus layer, which clogs the airways and traps bacteria leading to infections, extensive lung damage and eventually, respiratory failure. Most treatments like antibiotics and mucus-clearing agents are symptomatic and hence there is a great need for disease modifying agents.[3]

More than 2,000 mutations of the CFTR gene are known.[4] These CFTR defects have been grouped in 6 classes based on their defective mechanisms.[5] The most common mutation, F508del, belongs to the class II trafficking defects, where folding of the CFTR protein is impaired, resulting in a reduction of the

amount of ion channel present on the cell surface. With the G551D mutation (class III), the amount of protein is not affected but its open probability (P_o) is reduced,[6] resulting as well in a reduced channel gating. To address the underlying causes of cystic fibrosis, two biomolecular activities are required, namely correctors to increase CFTR levels at the cell surface, and potentiators to allow the effective opening of the CFTR channel.[3] For patients with the F508del mutation, a combination of correctors and potentiator will be necessary to restore CFTR function. For patients with the G551D mutation, a potentiator alone has been shown to be effective. In 2012, **1** (Ivacaftor) was approved as a monotherapy for patients who carry the G551D mutation[7] and has recently been approved for additional mutations influenced by a potentiator alone.[8] This was followed in 2015 by the approval of Orkambi, a combination of Ivacaftor and the corrector 3-[6-[[1-(2,2-difluoro-1,3-benzodioxol-5-yl)cyclopropanecarbonyl]amino]-3-methyl-2-pyridyl]benzoic acid (VX-809), for cystic fibrosis patients with 2 copies of the F508del allele.[9] This treatment results in only minor benefit to the patients and thus there is a demand for more effective therapies to further improve clinical benefit for CF patients with the F508del mutation.[10]

RESULTS AND DISCUSSION

To check for compounds which can restore chloride transport mediated by the CFTR ion channel, a CFTR dependent yellow fluorescent protein (YFP) halide assay was developed. A bronchial epithelial cell line derived from a CF patient (CFBE41o- cells) was used to overexpress F508del CFTR and yellow fluorescent protein.[11] In order to have enough F508del CFTR on the membrane, cells were incubated at 27°C. Alternatively, activity on different class III and IV mutants was measured in HEK293 cells, expressing the respective mutant CFTR and YFP. The CFTR activity is proportional to the quenching of the YFP related fluorescence and the % activation is a measure for the extent or efficacy of channel opening.

The search for novel potentiators started by performing a screen on 589 commercial compounds which were selected based on similarity around existing potentiators (Figure 1. Overview potentiators).

From this screen, the most active hits were found around compound **2** (P5, Figure 1), a potentiator described by Verkmann et al.[12] Relative to Ivacaftor, the hit showed good starting potencies on F508del CFTR but failed to restore the chloride transport through G551D CFTR (Figure 2). In terms of molecular properties, the compound was perceived as a low molecular weight starting point, albeit having a calculated lipophilicity XLogP3 >4.[13] In line with the lipophilic nature of the compound, it showed high unbound clearance in the rat liver microsomal stability assay.[14]

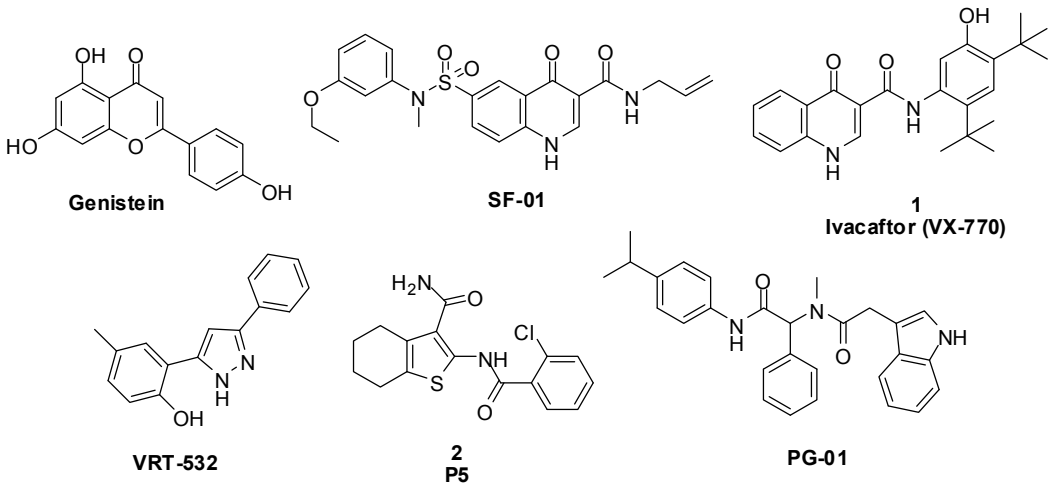

Figure 1. Overview potentiators. Genistein has been used as a general tool compound.[15] Compounds sulfonamide-01 (SF-01)**,** phenylglycine-01 (PG-01) and **2** were described by Verkmann et al. to have potentiating activites.[16,12] Phenyl-pyrazole (VRT-532) has been disclosed by Vertex Pharmaceuticals.[17]

In terms of chemical exploration, **2** was considered as an interesting starting point. The core was readily built up by a Gewald reaction (Scheme 2), allowing exploration of different scaffolds by simply varying the starting ketone. Keeping the high rat microsomal clearance in mind, initial exploration focused at installing a hetero-atom into the cyclohexyl ring to improve the unbound clearance.

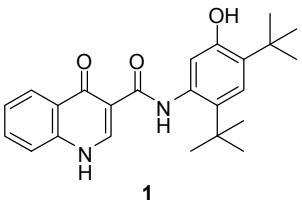

1
Ivacaftor

F508del: 126nM, 100%
G551D: 1300nM, 50%
MW/xLogP/PSA: 393/5.59/78

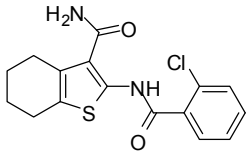

2

F508del: 326nM, 71%
G551D: >10μM, 18%
MW/xLogP/PSA: 335/4.1/100
Clint,unb,μsome,rat (L/h/kg): 84

Figure 2. Comparison of **2** with **Ivacaftor**.

Introduction of a basic nitrogen resulted in the loss of activity (Table 1, **4**). The ether analogue **5** showed activity comparable to **3** but with an improved polarity. Further potency improvements were made by introducing steric bulk next to the oxygen atom (**6**, **7** and **8**). Compound **6** was the least potent while **7** and **8** had similar potencies and efficacies on the F508del mutant. On G551D CFTR however, **8** was more efficacious in opening the ion channel as represented by the higher % activation. Therefore, the tetramethyl-tetrahdyropyran (THP) scaffold was chosen for as the starting point for further exploration.

Table 1. Activity in YFP halide assay of selected compounds.

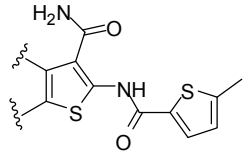

A

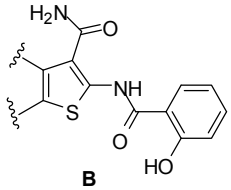

B

Cmpd	R	Amide group	XLogP3	F508del EC_{50}, % activity	G551D EC_{50}, % activity
3		**A**	3.8	652nM, 72%	-
4		**A**	2.1	NA, 3%	-
5		**A**	2.3	778nM, 74%	-
6		**B**	2.7	13nM, 93%	490nM, 51%
7	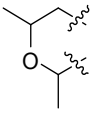	**B**	3.0	4nM, 98%	236nM, 36%
8	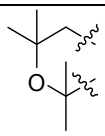	**B**	3.3	4nM, 111%	162nM, 52%

Using the novel tetramethyl-THP scaffold, the amide SAR was more thoroughly explored. Although **8** had good potency and efficacy on the 2 tested CFTR mutants, the phenolic moiety was considered as an issue because of the risk of phase II metabolism. A broad exploration was undertaken, but in general it appeared that groups containing a proton donor were consistently more active. Table 2 summarizes the SAR collected by targeting groups containing an acid proton, mimicking the phenol group of **8**. Close isosters like **9** and **10** showed a >40 fold loss in potency. Installing small heterocycles with an acidic proton like the triazole **11** showed an even greater loss in potency. The pyrazole **12** also was much less

active, but its isomer **13** appeared to very active on the F508del mutant. The elongated compound **14** had similar activity to **12**, showing that the position of the proton donor and acceptor as present in **13** is crucial for good activity.

Table 2. Activity in YFP halide assay on F508del CFTR of selected amides.

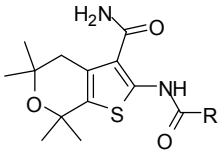

Cmpd	R	F508del EC_{50} (nM)	Cmpd	R	F508del EC_{50} (nM)
9	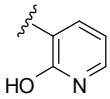	190	**15**	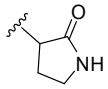	101
10	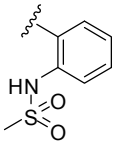	147	**16**	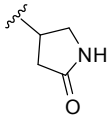	>10,000
11		467	**17**		23
12	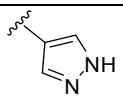	125	**18**		16
13	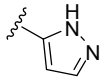	3	**19**	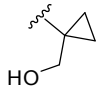	15
14	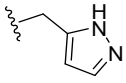	136	**20**		75

In effort to increase the fraction sp^3(fsp^3),[18] lactams and saturated alcohols were explored to see whether the H-bonding pattern present in **8** and **13** could be mimicked. In this case, a big difference in potency between the 2 lactam isomers **15** and **16** was observed. Nevertheless, **15** still showed a > 30 fold loss in potency compared to **13**. More successfully, alcohols **17, 18** and **19** showed good potencies

<25 nM. In contrast to the sharp difference in potency between **12, 13** and **14**, it seemed that the position of the alcohol was less crucial.

From this amide exploration, 2 subseries emerged as being very promising, namely the pyrazoles and alcohols. These were further expanded and profiled against both the F508del and the G551D CFTR mutant.

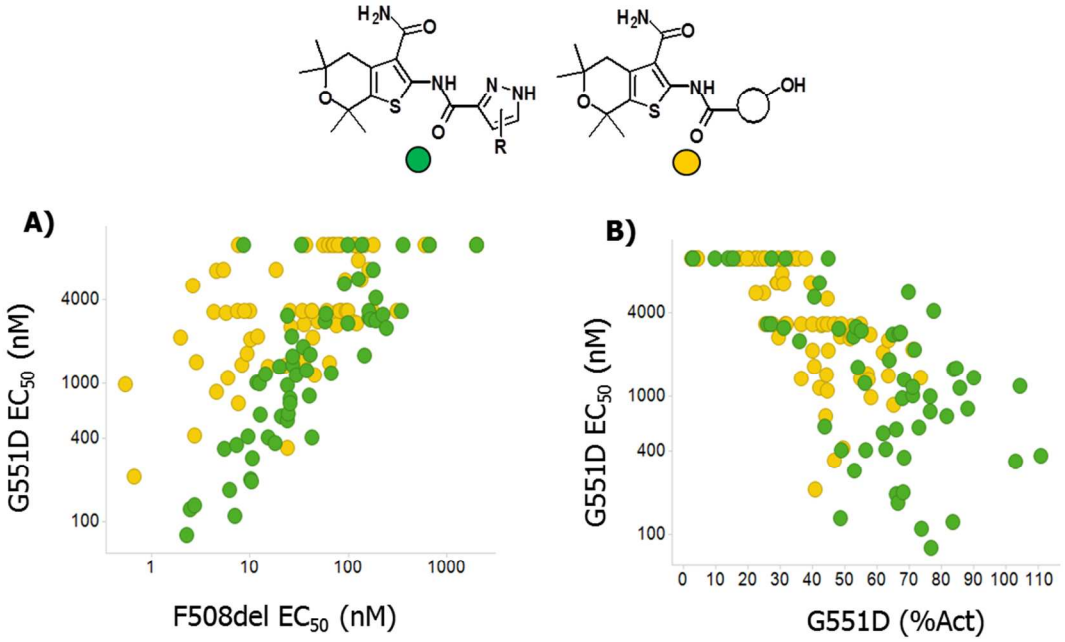

Figure 3. YFP halide assay profiling of the alcohol and pyrazole subseries on the F508del and G551D CFTR. Green dots represent pyrazoles and yellow dots alcohols. A) shows the potencies against F508del and G551D CFTR. B) shows the correlation between the potency and efficacy on the G551D CFTR for both subseries.

For both subseries, it was possible to get to compounds with potencies <10 nM on the F508del CFTR. For the F508del mutation, the % activation, a measure for the extent or efficacy of channel opening, was between 90-110% (data not shown) for most compounds. Although there was a good correlation between the potencies for F508del and G551D, most of the compounds were in general less potent for the G551D than for the F508del CFTR. This is consistent with the erosion in potency of Ivacaftor for

F508del vs G551D CFTR (own data in Figure 2 and reference 6c). Whereas it was difficult to discriminate the 2 subseries based on their F508del profile, the pyrazole subseries consistently showed to be more potent and more effective in opening the G551D CFTR channel (Figure 3). Indeed, it looked as if the alcohol subseries was less effective in opening the G551D CFTR. This is represented best with alcohol **23** in Table 3. Although the compound had a sub-nanomolar potency on F508del, it was only 981 nM on G551D, reflecting almost a 2000 fold loss in potency. In addition, the % activation of **23**, but also the other alcohols **19**, **21** and **22**, was significantly lower than most pyrazoles. Also, the chirality of the alcohols had a strong impact on the potency. The 'S' enantiomer **21** is 47 and 18 times more potent on F508del and G551D CFTR respectively than its 'R' isomer.

Starting from pyrazole **13**, the SAR around the heterocycle was further explored. In general, substitution on the pyrazole either on the 3 or 4 position, did improve the potency for G551D CFTR 2 to 4 fold (**24**, **25** and **26**). For F508del CFTR, no benefit was obtained with these substitutions. However, improving the potency did coincide with a reduction in efficacy. Compound **26** was the most striking example with an efficacy reduced to 49%. These changes did not influence potency on F508del CFTR. Double substitution as in the case of **28** resulted in a similar profile as the mono-substituted pyrazoles.

Table 3. Summary of the SAR around the alcohols and pyrazoles.

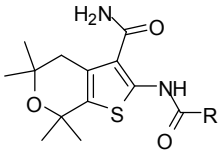

Cmpd	R	F508del EC_{50}, % activity	G551D EC_{50}, % activity	Cmpd	R	F508del EC_{50}, % activity	G551D EC_{50}, % activity
19	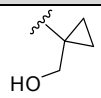	15 nM, 105%	1,320 nM, 57%	**13**	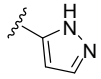	3 nM, 105%	339 nM, 103%
21		2.7 nM, 95%	421 nM, 50%	**25**	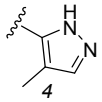	2 nM, 96%	123 nM, 83%
22		127 nM, 95%	7,777 nM, 31%	**26**	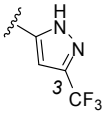	3 nM, 107%	130 nM, 49%
23	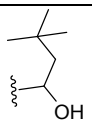	0.54 nM, 102%	981 nM, 58%	**27**	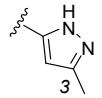	13 nM, 81%	590 nM, 73%
24	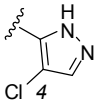	2 nM, 96%	81 nM, 77%	**28**	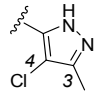	11 nM, 92%	199 nM, 68%

In the end, **13** showed to have the most interesting profile, having an EC_{50} of 3 nM and 339 nM on F508del and G551D CFTR respectively. Upon benchmarking **13** against Ivacaftor, which had an efficacy of 50% (Figure 2) for G551D CFTR, it seemed that **13** was twice as efficacious as Ivacaftor in the YFP halide G551D assay. This observation was confirmed in a Trans-epithelial Clamp Circuit (TECC)[19] assay using primary patient cells. The increased conductivity of the G551D CFTR channel by compound **13** was nearly 200% compared that of Ivacaftor (Figure 4). The obtained potency of **13** was 181 nM. This is the first time, to our knowledge, that a novel potentiator is reported that shows an improved potency and

efficacy in G551D primary human bronchial epithelial (HBE) cells compared to the current standard of care Ivacaftor. A detailed mechanistic study has been published recently, showing that **13** increases the P_0 of CFTR .[20]

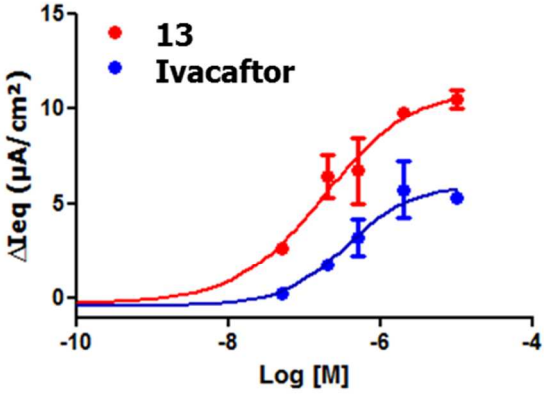

Figure 4. G551D/F508del HBE cells treated with **Ivacaftor** and **13**.

This feature of improved conductivity was further investigated on the class III gating mutations G178R, S549N and the class IV conductance mutation R117H For these mutant CFTR forms, it has been shown that the addition of Ivacaftor can restore CFTR function.[8,21]. In many (but not all) cases the tetramethyl-THP potentiators were able to improve the defect to a greater extent when compared to Ivacaftor (Figure 5). Compound **13** was on all mutations more potent and showed a higher efficacy when compared to Ivacaftor. The extent of the increased efficacy varies between the different mutations (158% for G178R, 143% for S549N and 119% for R117H).

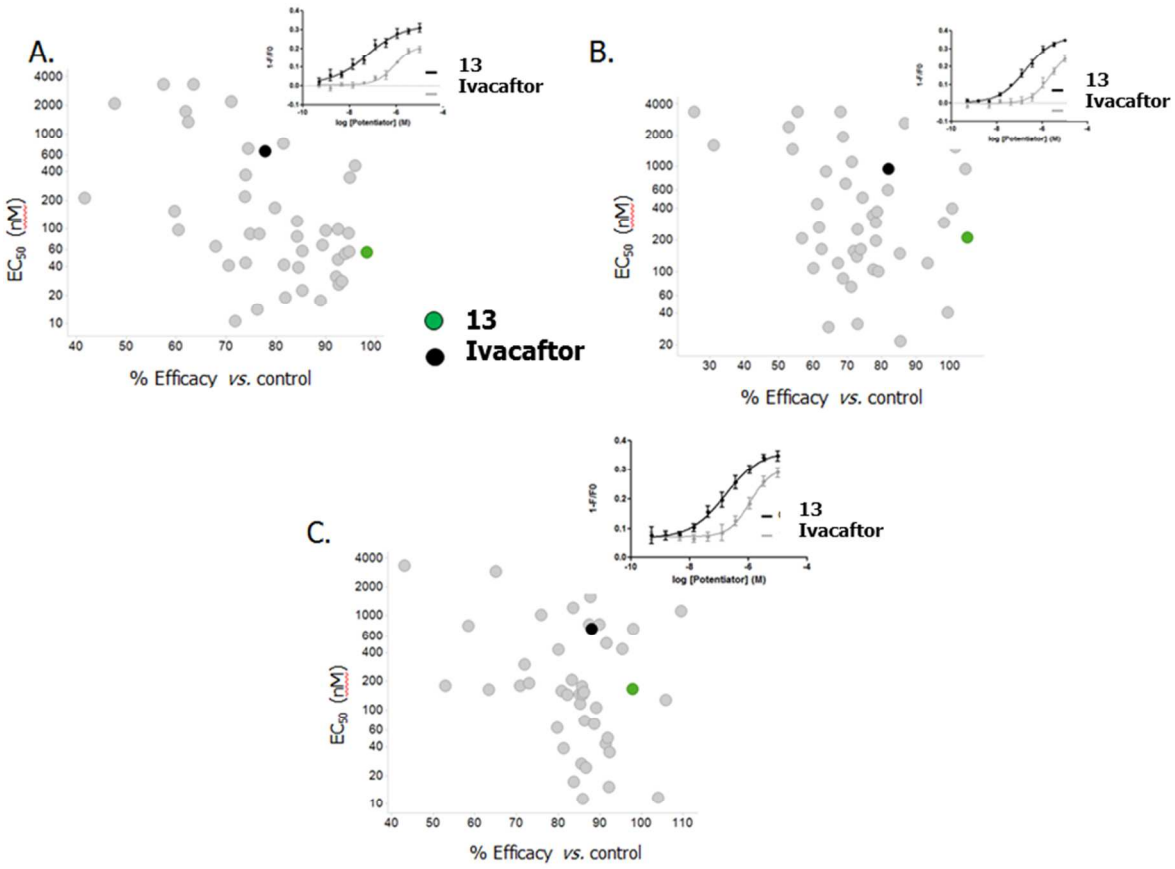

Figure 5. Progression of potency (Y-axis) and efficacy (% activation to control, X-axis) of potentiator series on various CFTR mutants (A. G178R; B. S549N, C. R117H) in YFP halide assay. Top right corner of each panel shows dose response curve of **13** (black) and **Ivacaftor** (grey).

Compound **13** had an attractive in vitro ADME profile, showing low Clint,unb in both microsomal and hepatocytes stability assays, good permeability and no off target inhibition of CYPs and the hERG channel (Table 4). On the other hand, the thermodynamic solubility was low at neutral and acidic pH, but this did not limit the bioavailability (F%) at the 5 mg/kg dose. Moreover, the pharmacokinetic profile of **13** was attractive, showing a low Cl,unb and good F% in both rat and dog (Table 5).

Table 4. Physicio-chemical and *in vitro* ADME parameters for **13.**

MW/XLogP/PSA/Fsp3	348 / 1.8 / 138 / 0.44
Clint,unb, µsome (L/h/kg) (r,h)	1.7 / 1.1
Clint,unb, hep (L/h/kg) (r,h)	5.7 / 1.8
CYP inhibition (1A2, 2C19, 2C9, 2D6, 3A4) (EC_{50}, µM)	>100 for all tested CYPs
hERG (manual Patch Clamp, EC_{50} µM)	>33
Thermodynamic ASOL (pH 7.4, 3.0) (µM)	8.6 / 11
MDCK (A2B $cm.10^{-6}sec^{-1}$, Efflux ratio)	11 / 2.6

Table 5. Pharmacokinetic properties of **13** in rat and dog. IV parameters were determined using a 1 mg/kg dose. F% was determined after a PO dose of 5 mg/kg.

	Cl (L/h/kg)	Cl,unb (L/h/kg)	Vd (L/kg)	T1/2 (h)	F%
Rat PK	1.92	24	4.8	1.84	67
Dog PK	0.32	6.4	1.4	3.0	>100

However, due to the low thermodynamic solubility, the observed exposures at 100mg/kg and 300 mg/kg in rat were lower than expected (data not shown). The calculated lipophilicity of **13** was 1.8, indicating that the low solubility was not originating from the lack of polarity and related poor solvation ('grease ball molecules').[22] On the contrary, with a melting point of >300°C, **13** could be considered as a 'brick dust' molecule. The crystal lattice seemed to be stabilized by strong inter-molecular hydrogen bonds originating from the carboxamide and the pyrazole ring (Figure 6**Error! Reference source not**

found.). Both groups are a donor-acceptor pair in terms of hydrogen bonding, allowing efficient hydrogen bonding with a donor-acceptor

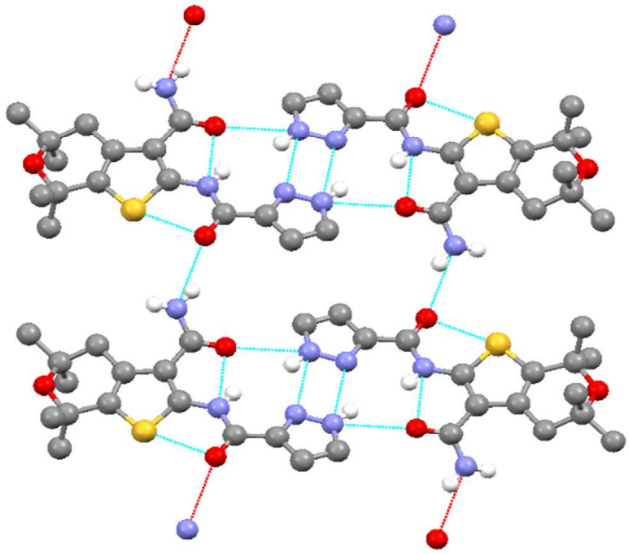

Figure 6. X ray structure of **13**. Sulfur atoms are coloured yellow, oxygens red, nitrogens blue, carbons grey and hydrogen white.

pair from another molecule. The X ray analysis also showed that there was extensive intra-molecular bonding. Not surprisingly, the 2 amides in the molecule were locked up by an internal hydrogen bond. Additionally, the carbonyl of the amide *ortho* on the thiophene ring, was held planar by an intra-molecular interaction where the carbonyl electrons were interacting with the electrophilic sulfur atom of the thiophene ring.[23] This explained why a compound with high PSA value of 138, still had very good permeability as measured in the MDCK assay (Table 4). Due to the intra-molecular interactions, one hydrogen bond donor and 2 hydrogen bond acceptors are shielded, lowering the effective PSA.

In order to improve the solubility, a phosphate prodrug strategy was applied (Scheme 1). This approach is well documented and has proven to improve solubility and exposure for a range of compounds administered by either an intravenous (IV) or oral (PO) route.[24] The phosphate prodrug is selectively cleaved in the gut by alkaline phosphatases, located at the brush border of the epithelial cells.[25] Upon

cleavage, formaldehyde and the parent compound are released.[26] In addition of improving the solubility, the phosphate prodrug has the advantage of only having the parental compound systemically exposed. In all PK experiments performed with the prodrug **29**, the prodrug could never be detected in the plasma.

Scheme 1. Phosphate prodrug **29** and its mechanism of cleavage

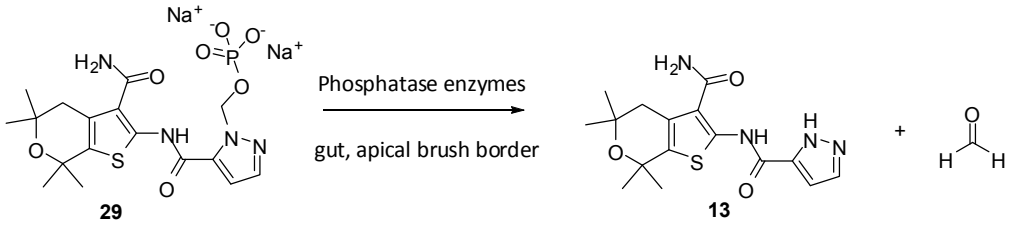

29 13

When comparing the exposure of **13** via its prodrug **29**, it seemed that at 5 mg/kg, there was no difference in obtained Cmax and AUC. This implies, that at the lower dose, the low solubility of **13** is not limiting its exposure. On the other hand, an increase in both Cmax and AUC was observed when dosing 300mg/kg, showing that the phosphate prodrug strategy was effective at addressing the low solubility and low F% at higher doses.

In a parallel effort, various solid state formulations were explored and in the end, a nanosuspension of **13** was developed leading to similar results as obtained with **29** (data not shown).

Table 6. Pharmacokinetic properties of **13** in rat at higher doses. Comparison of the AUCs of **13** obtained after administration of the parental compound directly, or the prodrug **29** is given.

	13	**13 via prodrug 29**
Rat PK (5mg/kg) Cmax (ng/ml)/ AUC (ng*hr/ml))	331/1,540	741/1,562
Rat PK (300mg/kg) Cmax (ng/ml)/ AUC (ng*hr/ml))	4,674/68,170	12,378/192,264

With an improved formulation in hand, **13** was nominated as **GLPG1837** and selected for pre-clinical safety evaluation after which it was progressed into a phase I study to evaluate its PK and safety in humans. Compound **13** was generally safe and well tolerated in healthy volunteers, with single doses up to 2000 mg and 14-day dosing up to 800mg b.i.d. The efficacy was explored in 2 phase II studies the SAPHIRA I and SAPHIRA II, for which data will be reported soon.

CHEMISTRY

Scheme 2. Synthesis of the main scaffold **31** by a Gewald reaction[a]

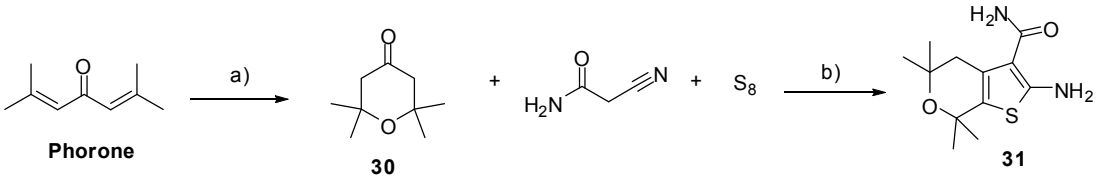

[a]Reagents and conditions: (a) 1M HCl, 40°C, 6 days, 45%; (b) S8, diethylamine, EtOH, 40°C, 18h, 35%.

The core **31** was synthesized by a multi-component Gewald reaction (Scheme 2) in which the ketone **30** reacts with sulfur and cyanoacetamide in the presence of a base.[27] Although **30** was commercially available, the first large quantities were prepared by stirring the readily available Phorone at 40°C in acidified water.

Derivatisation of the scaffold **31** was done by amide bond formation. It was found that the Mukaiyama reagent (2-chloro-1-methylpyridinium iodide, CMPI[28]) gave the most consistent results, allowing the coupling of great variety of different amides (Scheme 3).

Scheme 3. Synthesis of pyrazole derivatives using the Mukaiyama reagent[a]

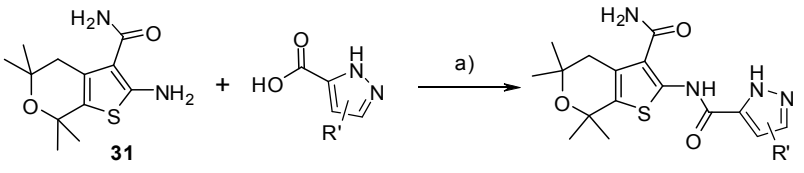

[a]Reagents and conditions: (a) 2-chloro-1-methylpyridinium iodide, DMAP, TEA, DCM, 50°C, 2h.

For the synthesis of the alcohols, generally the alcohol function needed to be masked to guarantee a successful amide coupling. One option was to couple the corresponding ketone or ester, followed by reduction (Scheme 4). Alternatively, the alcohol was first protected, before engaging into the amide coupling. This is exemplified for compound **21** in Scheme 5. Here, an acetate protecting group was used which could be subsequently removed by hydrolysis.

Scheme 4. Synthesis of alcohol **19**[a]

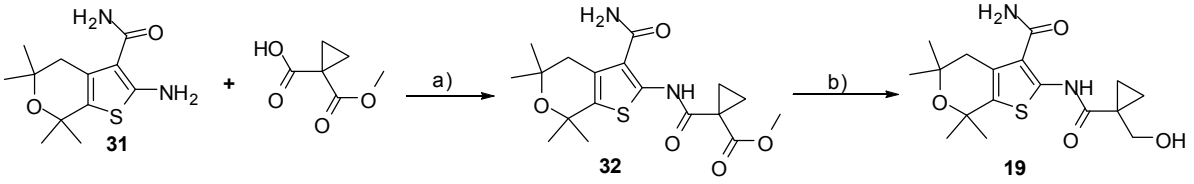

[a]Reagents and conditions: (a) 2-chloro-1-methylpyridinium iodide, DMAP, TEA, DCM, 50°C, 2h; (b) $LiBH_4$, dry THF, 0° -> rT, 32%.

Scheme 5. Synthesis of alcohol **21**[a]

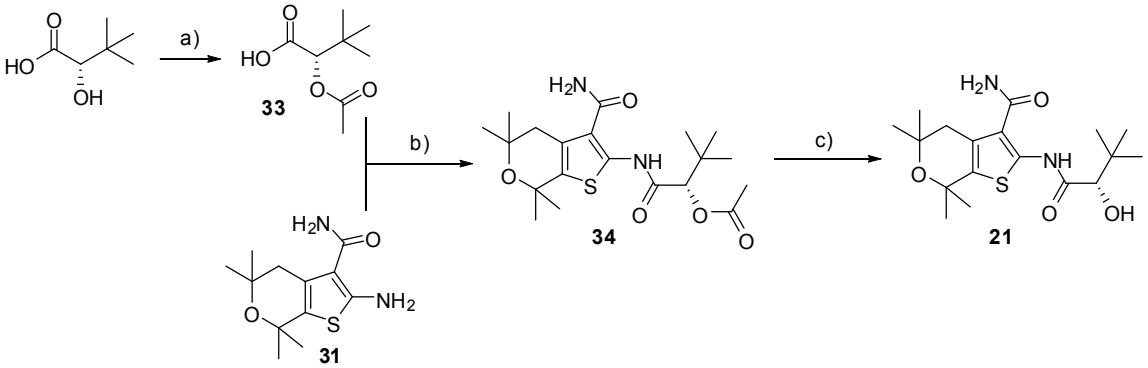

[a]Reagents and conditions: (a) ethanoly chloride, pyridine, DCM, 0°C - rT (b) 2-chloro-1-methylpyridinium iodide, DMAP, TEA, DCM, 40°C, 16h (c) $LiOH.H_2O$, THF, water, 40°C, 16h.

For the synthesis of the phosphate prodrug **29**, the di-tert-butyl chloromethyl phosphate group was introduced on the pyrazole ester by alkylation (Scheme 6). This gave rise to two regio-isomers that could be separated by column chromatography. Hydrolysis with LiOH gave the corresponding acid that was coupled to **31** using the Mukaiyama reagent. Once coupled, the tBu protecting groups were removed under very mild conditions.

Scheme 6. Synthesis of the phosphate prodrug 29[a].

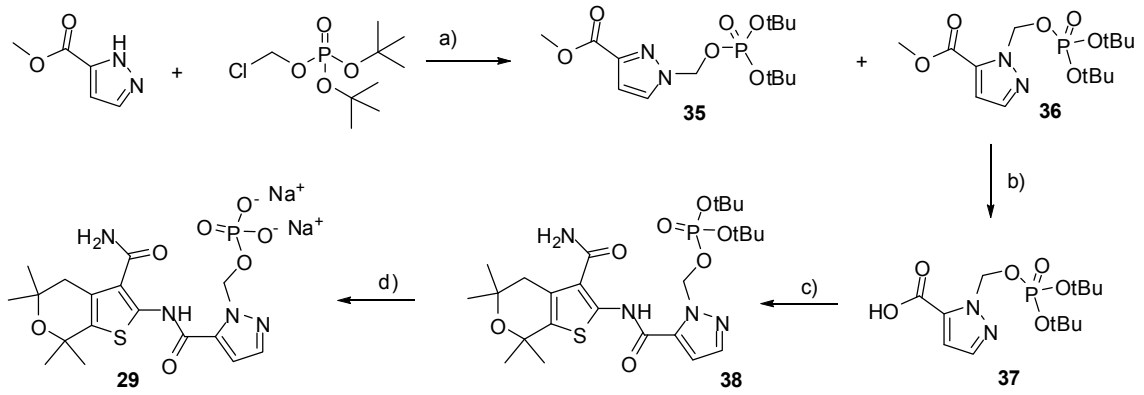

[a]Reagents and conditions: (a) Cs_2CO_3, DMA, 55°C, 35% after column chromatography; (b) LiOH (1 M), THF/MeOH/H2O, 45°C, 99%; (c) 31, Mukaiyama reagent, DMAP, Et_3N, DCM, 45°C, 99%; (d) acetone/water, 45°C, 51%.

CONCLUSION

Starting from the described potentiator **2** a novel potentiator series was discovered using the tetra-methyl-THP scaffold. In contrast to **2**, the novel series was able to efficiently potentiate G551D CFTR. During lead optimization, two subseries (alcohols and pyrazoles) were thoroughly explored. Upon benchmarking against Ivacaftor, it seemed that the pyrazole subseries consistently showed an improved restoration of the channel activity of G551D CFTR. In the end, the best efficacy was obtained with the unsubstituted pyrazole **13.** The enhanced efficacy was confirmed with a Tecc experiment on primary human G551D/F508del bronchial epithelial cells. Here, **13** not only induced a current which was almost 200% compared to Ivacaftor, but was in the same time also more potent. Hence, **13** represents a novel potentiator with improved potency and efficacy compared to the current standard of care, Ivacaftor. Phase II evaluation of **13** in patients recently finished and data will be reported soon.

EXPERIMENTAL SECTION

Yellow Fluorescent Protein (YFP) halide assays

CFBe41o- cells were cultured in Eagle's minimal essential medium (MEM) (Life Technologies) supplemented with 10 % fetal bovine serum (FBS), 1 % penicillin/streptomycin, 1 % L-glutamine and 500 µg/ml hygromycin B. The cells were grown on culture flasks coated with 0.01 % bovine serum albumin (BSA) (Sigma), 30 µg/ml Purecol (Nutacon) and 0.001 % human fibronectin (Sigma). CFBe41o- cells were transduced with adenoviruses containing F508del CFTR and YFP (H148Q/I152L/ F47L). HEK293 cells were cultured in Dulbecco's Modified Eagle Medium (DMEM) (Life Technologies) supplemented with 10% FBS and 1 % penicillin/streptomycin. HEK293 cells were transfected with plasmids containing G551D, G178R, , S549N, R117H, CFTR and YFP (H148Q/I152L/F47L). Directly after transfection, the HEK293 cells were seeded in black 96-well plates coated with Poly-D-lysine at a density of 70,000 cells per well. The next day, cells were incubated for 24h at 27°C (CFBE41o-) or 37°C (HEK293). Then, cells were treated for 10 min with 10 µM forskolin and the desired concentration of potentiator at room temperature. The YFP fluorescence was recorded during 7 s (CFBE41o-) or 2 min (HEK293), starting immediately before addition of NaI buffer (CFBE41o-: 137 mM NaI, 2.7 mM KI, 1.7 mM KH2PO4, 10.1 mM Na2HPO4, 5 mM D-glucose, HEK923: (375 mM NaI, 7.5 mM KI, 1.76 mM KH2PO4, 10.1 mM Na2HPO4, 13.75 mM glucose) to the wells, using a fluorescence reader. The capacity of potentiators to increase CFTR channel function was expressed as 1-(fluorescence after NaI addition (F) / fluorescence before NaI addition (F0)).

TECC experiments

Trans-epithelial clamp circuit (TECC) recordings were performed using the TECC instrument developed and sold by EP Design (Bertem, Belgium). During the recording,the epithelia were bathed in a NaCl-Ringer solution (120 mM NaCl, 20 mM HEPES, 1.2 mM CaCl2, 1.2 mM MgCl2, 0.8 mM KH2PO4, 0.8 mM K2HPO4, 5 mM glucose, pH 7.4) on both the basolateral and the apical side and kept at 37°C. Apical amiloride was used to inhibit the endogenous epithelium sodium channel (ENaC) currents (100 µM)

while forskolin (10 μM) was applied on both the apical and basolateral sides to stimulate CFTR. For acute potentiator experiments, compounds were added on both sides to test their potential for increasing CFTR gating. Measurements were done during a 20-minute timeframe with recordings every 2 minutes. The transepithelial potential (PD) and transepithelial resistance (R_t) were measured in an open circuit and transformed to I_{eq} using Ohm's law. The increase in I_{eq} (Δ I) was used as a measure for the increased CFTR activity. EC50 values were generated by measuring impact of different concentrations of compound on I_{eq} in primary cells. For this purpose each transwell was treated with a different compound concentration. CFTRinh-172 was used at 10 μM to assess the specificity of the tested compounds. Each concentration of compound was tested in duplicate or triplicate, and average and standard error of the mean (SEM) were calculated.

Chemistry

All reagents were of commercial grade and were used as received without further purification, unless otherwise stated. Commercially available anhydrous solvents were used for reactions conducted under inert atmosphere. Reagent grade solvents were used in all other cases, unless otherwise specified. Column chromatography was performed on silica gel 60 (35-70 μm). Thin layer chromatography was carried out using pre-coated silica gel F-254 plates (thickness 0.25 mm). ^{1}H NMR spectra were recorded on a Bruker DPX 400 NMR spectrometer (400 MHz) or a Bruker Advance 300 NMR spectrometer (300 MHz). Chemical shifts (δ) for ^{1}H NMR spectra are reported in parts per million (ppm) the appropriate residual solvent peak, i.e. $CHCl_3$ (δ 7.27), as internal reference. Multiplicities are given as singlet (s), doublet (d), triplet (t), quartet (q), quintuplet (quin), multiplet (m) and broad (br). Microwave heating was performed with a Biotage Initiator.

Ultra-violet and electrospray MS spectra were obtained on a Waters Acquity H-Class UPLCwhich was coupled to a Waters Mass detector QDA or ZQ2000 and an Acquity PDA Detector (210-400nm). All final compounds reported were analyzed using one of these analytical methods and were at least 95% pure.

Columns used: Waters Acquity UPLC BEH C18 1.7µm, 2.1mm ID x 50mm L or Waters Acquity UPLC CSH C18 2.1x50mm 1.7 µm. The methods are using MeCN/H_2O gradients (H_2O contains either 0.1% TFA or 15 mM NH_3).

Racemic mixtures were separated on an Agilent HP1100 system with UV detection. Column used: Chiralpak 1A (10x250 mm, 5µm). Solvents used: iPrOH and tBME. Alternatively, separation was done using a SFC2 system. Column used: Lux Cellulose-4. Solvents used: CO2 and MeOH. Enantiomeric purity was determined on an Agilent HP1100 system with UV detection. Column used: Chiralpak IA (4.6x250 mm, 5µm). Solvents used: iPrOH and tBME.

N-(3-carbamoyl-5,5,7,7-tetramethyl-5,7-dihydro-4H-thieno[2,3-c]pyran-2-yl)-1H-pyrazole-5-carboxamide (13). Compound **31** (15 g, 59 mmol) and 2H-pyrazole-3-carboxylic acid (9.9 g, 88 mmol) were suspended in DCM (250 mL). Next, Mukaiyama reagent (2-chloro-1-methylpyridinium iodide) (18.1 g, 71 mmol), TEA (24.7 mL, 177 mmol) and DMAP (3.6 g, 29 mmol) were added. The reaction mixture was stirred at 40°C overnight and then cooled. The mixture was evaporated and the obtained crude was suspended in a 1 M HCl solution. After stirring for 10 min, the suspension was filtered and obtained precipitate was isolated. This precipitate was re-suspended in a 0.1 M citric acid solution. Again, filtration gave a precipitate. A third trituration was done using ether as a solvent to give a precipitate after filtration. Finally, the precipitate (13.6 g) was suspended in EtOH (816 mL) and heated at reflux. To this suspension, 65 mL of DMF was added and a clear solution was obtained. The solution was concentrated to 275 mL and cooled at 0°C. A suspension was obtained, the solid was separated by filtration, and the cake was dried affording the desired product. ^{1}H NMR δ (ppm)(DMSO-d6) : 13.55 (1 H, s br), 12.53 (1 H, s br), 7.94 (1 H, s br), 7.54 (1 H, s br), 7.10 (1 H, s br), 6.79 (1 H, s), 2.73 (2 H, s), 1.45 (6 H, s), 1.20 (6 H, s), 1.45 (6 H, s). LC−MS: m/z = 371 $[M + Na]^+$.

2-(1-(hydroxymethyl)cyclopropanecarboxamido)-5,5,7,7-tetramethyl-5,7-dihydro-4H-thieno[2,3-c]pyran-3-carboxamide (19). Compound **31** (2 g, 7.9 mmol) was mixed with dimethyl 1,1-

cyclopropanedicarboxylate (CAS: 6914-71-2, 1.33 g, 10.2 mmol), DMAP (480 mg, 3.9 mmol), Mukaiyama reagent (2.4 g, 9.4 mmol) and triethylamine (3.3 mL, 24 mmol) in DCM (25 mL) under N_2. The mixture was stirred at 40°C overnight, after which the mixture was evaporated. A yellow precipitate was obtained that was suspended in water. Subsequent filtration gave a yellow powder. This was re-suspended in 0.1 M HCl_{aq}, followed by filtration to give an off-white solid. The obtained solid was dissolved in DCM and dried over $MgSO_4$. In the end, 3.4 g (113%) of compound **32** was obtained which was used as such. LC-MS: m/z = 381 [M+H].

Compound **32** (100 mg, 0.26 mmol) was weighed together with $LiBH_4$ (17 mg, 0.79 mmol) in a flask. The flask is put in an ice bath and dry THF (2 mL) was slowly added. After stirring for 5 min, the ice bath was removed and the mixture was stirred at room temperature. Reaction was subsequently quenched with 2 M HCl, diluted with water and extracted with EtOAc. The organic phase was evaporated and the obtained residue was purified by preparative chromatography, yielding 29 mg white powder (32%). ^{1}H NMR δ (ppm)(400 MHz,$CDCl_3$): 12.42 (s, 1H), 5.74 (br. s., 2H), 3.81 (d, *J* = 4.9 Hz, 2H), 3.02 (t, *J* = 5.0 Hz, 1H), 2.64 (s, 2H), 1.49 (s, 6H), 1.32 - 1.40 (m, 2H), 1.27 (s, 6H), 0.84 - 0.92 (m, 2H). LC–MS: m/z = 353 [M + H].

2-[[(2S)-2-hydroxy-3,3-dimethyl-butanoyl]amino]-5,5,7,7-tetramethyl-4H-thieno[2,3-c]pyran-3-carboxamide (21). To a solution of (2S)-2-hydroxy-3,3-dimethyl-butanoic acid (0.76 g, 5.8 mmol) in dichloromethane (20 ml) were added successively pyridine (1 ml, 11.5 mmol) and ethanoyl chloride (drop wise, 821 µl, 11.5 mmol) at 0°C. The reaction mixture was stirred 1hour at room temperature. The mixture was diluted with water followed by extraction with dichloromethane. The combined organic layers were washed with water and brine, dried over Na_2SO_4, filtered and concentrated *in vacuo* to afford crude (2S)-2-acetoxy-3,3-dimethyl-butanoic acid (**33**) which was used as such in the next step. LC-MS: m/z= 175.1 [M+H].

Compound **31** (1.5 g, 5.8 mmol) was added to a solution of **33** **(**1.5 g, 5.8 mmol), 2-chloro-1-methylpyridinium iodide (2.2 g, 8.7 mmol), triethylamine (2.4 mL, 17.4 mmol) and 4-dimethylaminopyridine (350 mg, 2.9 mmol) in dichloromethane (40 mL). The resulting reaction mixture was heated at 40°C for 16 h. After cooling to room temperature, 10% citric acid aqueous solution was added and the reaction mixture was extracted with dichloromethane. The combined organic layers were washed with water and brine, dried over Na_2SO_4, filtered and concentrated in vacuo. to afford crude [(1S)-1-[(3-carbamoyl-5,5,7,7-tetramethyl-4H-thieno[2,3-c]pyran-2-yl)carbamoyl]-2,2-dimethyl-propyl] acetate (**34**) which was used as such in the next step. LC-MS: m/z= 411.2 [M+H].

Lithiumhydroxide monohydrate (486 mg, 11.6 mmol) was added to a solution of crude **34** (2.36 g, 5.8 mmol) in THF (15 ml) and water (3 ml). The reaction mixture was stirred for 16h at 40°C. Organic solvent was removed under reduced pressure and the remaining solution was acidified to pH = 1 with 1 N HCl_{aq} solution. The resulting mixture was extracted with DCM. The combined organic layers were washed with water and brine, dried over Na_2SO_4, filtered and concentrated in vacuo to afford crude 2-[[(2S)-2-hydroxy-3,3-dimethyl-butanoyl]amino]-5,5,7,7-tetramethyl-4H-thieno[2,3-c]pyran-3-carboxamide (**21**). Crude mixture was purified by column chromatography on silica gel (eluens: petroleum ether/ethyl acetate: 75/25) and subsequent crystallisation from EtOH to afford pure title compound (398 mg, 18%). LC-MS: m/z= 369.1 [M+H]. ^{1}H NMR δ (ppm)(DMSO-d6): 11.98 (s, 1H), 7.49 (br.s, 1H), 6.93 (br.s, 1H), 6.19 (d, *J* = 5.2 Hz , 1H), 3.73 (d, *J* = 5.2 Hz, 1H), 2.70 (d, 2H), 1.43 (s, 6H), 1.19 (d, *J* = 8.8 Hz, 6H), 0.93 (s, 9H).

Disodium phosphoric acid mono-[5-(3-carbamoyl-5,5,7,7-tetramethyl-4,7-dihydro-5H-thieno[2,3-c]pyran-2-ylcarbamoyl)-pyrazol-1-ylmethyl] ester (29). To a solution of phosphoric acid di-tert-butyl ester chloromethyl ester (46.2 g, 179 mmol) in DMA (425 mL) under N_2, 1H-pyrazole-3-carboxylic acid ethyl ester (25 g, 179 mmol) and Cs_2CO_3 (73 g, 223 mmol) were added (portion wise) at room temperature. The resulting turbid mixture was stirred at 55°C under N_2 overnight. Once reaction was finished (determined by LC-MS), the mixture was allowed to reach room temperature, added to water

(800 mL) and extracted with Et2O (~5x 200 mL). The combined organic fractions were washed with water/brine (~4x 500 mL), dried over Na_2SO_4 and concentrated in vacuo. The two regioisomers **35** and **36** were separated by means of silica chromatography (columns were pre-treated with Et_3N in petroleum ether to avoid deprotection of the tert-butyl groups) with a gradient (100% petroleum ether to 50% EtOAc in petroleum ether), yielding the targeted isomer **36** (17 g, 26%) which was identified via NOESY experiments (see SI). ^{1}H NMR (400 MHz, DMSO-d6) δ (ppm) 8.03 (d, *J* = 2.5 Hz, 1H), 6.81 (s, 1H), 5.90 (d, *J* = 11.6 Hz, 2H), 4.28 (q, *J* = 7.1 Hz, 2H), 1.37 (s, 18H), 1.28 (t, *J* = 7.1 Hz, 3H). LC-MS: m/z = 363 [M+H].

To a solution of 2-(di-tert-butoxy-phosphoryloxymethyl)-2H-pyrazole-3-carboxylic acid ethyl ester **36** (18.6 g, 51.3 mmol) in THF/MeOH/H_2O (270 mL, 54 mL, 54 mL), LiOH (1.29 g, 53.9 mmol) was added. The resulting mixture was stirred at 45°C under N_2 for 2 hours. After cooling down, mixture diluted with water and acidified to pH=3-4 (HCl, 2M). Aqueous phase was extracted with Et_2O whilst maintaining pH at 3-4. The combined organic fractions were dried over Na_2SO_4 and concentrated *in vacuo*. Compound **37** was obtained as a white solid (17 g, 99%) and used as such in the next reaction. LC-MS: m/z = 335 [M+H].

To a solution of **37** in CH_2Cl_2 (350 mL), 2-chloro-1-methylpyridinium iodide (17.7 g, 69.3 mmol), 4-dimethylaminopyridine (7.06 g, 57.8 mmol) and Et_3N (12.1 mL, 13.1 mmol) were added at room temperature. The resulting suspension was stirred for 10 minutes at room temperature, after which **31** was added and finally heated at reflux for 24 hours under N_2. After completion, reaction was cooled down, added to water and extracted with CH_2Cl_2. Combined organic fractions were washed with HCl (0.1M, 2x), dried over Na_2SO_4 and concentrated *in vacuo*, yielding **38** as a dark red viscous oil which was used as such. LC-MS: m/z = 571 [M+H].

To a solution of **38** (26.5 g, 46.4 mmol) in acetone (280 mL), water (280 mL) was added. The resulting mixture was stirred at 45°C in a RB flask under N2 for 24 h, after which the mixture was alkalized with NaOH (5M) to pH=~10. The aqueous mixture was washed with Et_2O twice, acidified to pH=~2 (HCl, 2M) and finally extracted with EtOAc. During extraction a precipitate was formed which was collected via filtration and combined with the concentrated organic fractions. The resulting solid was taken up again in water (100 mL), filtered and rinsed with water, Et_2O and acetone, yielding the title product as a white solid (10.8 g, 51%). ^{1}H NMR (400 MHz, DMSO-d6) δ (ppm) 12.65 (s, 1H), 7.78 (d, *J* = 2.0 Hz, 1H), 7.68 (s, 1H), 7.22 (s, 1H), 6.90 (d, *J* = 2.0 Hz, 1H), 6.18 (d, *J* = 8.3 Hz, 2H), 2.75 (s, 2H), 1.47 (s, 6H), 1.22 (s, 6H). LC-MS: m/z = 459 [M+H].

2,2,6,6-tetramethyltetrahydro-4H-pyran-4-one (30). Phorone or 2,6-dimethyl-2,5-heptadien-4-one (CAS: 504-20-1, 750 g) was mixed with an aqueous 1 M HCl solution (8 L) and the obtained emulsion is stirred at 40°C for 6 days. The water phase is extracted with DCM, and the organic phase is concentrated and purified by distillation to afford the desired product as an oil (448.8 g, 45%). ^{1}H NMR ($CDCl_3$):2.42 (s, 4H), 1.39 (s, 12H). GC-MS: m/z= 141 [M-$CH_3^{\bullet}$].

2-Amino-5,5,7,7-tetramethyl-4,7-dihydro-5H-thieno[2,3-c]pyran-3-carboxylic acid amide (31). To a flask containing **30** (32.3 g, 206.8 mmol), cyanoacetamide (17.4 g, 208 mmol) and sulfur (6.0 g, 186.1 mmol) were stirred in EtOH (85 mL). Diethylamine (23.5 mL, 227.4 mmol) was added and the reaction was stirred at 40°C overnight. The reaction was diluted with water (200 mL) and partially concentrated by evaporation causing the precipitation of a solid that is separated by filtration. The cake is then washed with water (2 x 150 mL) to afford the desired product (18.4 g, 35%). ^{1}H NMR (DMSO-d6): 6.80 (s, 1H), 6.51 (br. s., 1H), 2.49 (s, 1H), 1.25 (s, 3H), 1.10 (s, 3H). LC-MS: m/z= 238 [M-H_20]$^+$

ASSOCIATED CONTENT

Preparation and characterization for additional final compounds, NOESY analysis of **35** and **36** are available at http://pubs.acs.org.

AUTHOR INFORMATION

Corresponding Authors

*Steven E. Van der Plas: phone, +3215342900; e-mail: steven.vanderplas@glpg.com

*Katja Conrath: phone, +3215342900; e-mail: katja.conrath@glpg.com

REFERENCES

[1] https://www.cff.org/What-is-CF/About-Cystic-Fibrosis, last accessed on Nov 13, 2017.

[2] (a) Lubamba, B.; Dhooghe, B.; Noel, S.; Leal, T. Cystic fibrosis: insight into CFTR pathophysiology and pharmacotherapy. *Clin Biochem.* **2012**, *15*, 1132-1144. (b) Hanrahan, J. W.; Sampson, H. M.; Thomas, D. Y. Novel pharmacological strategies to treat cystic fibrosis. *Trends Pharmacol Sci.* **2013**, *34*, 119-125. (c) Merk, D.; Schubert-Zsilavecz, M. Repairing mutated proteins--development of small molecules targeting defects in the cystic fibrosis transmembrane conductance regulator. *Expert Opin Drug Discov.* **2013**, *8*, 691-708. (d) Riordan J.R.; Rommens J.M.; Kerem R.S.; Alon N.; Rozma-Hel R.; Grzel- czak Z.; Zielenski J.; Lok S.; Plavsic N.; Chou J.L.; Drumm M.L.; Iannuzzi C.; Collins F.S.; Tsui L.C. Identification of the cystic fibrosis gene: cloning and characterization of complementary DNA. *Science* **1989**, *245*, 1066– 1073.

[3] (a) Schmidt, B.; Haaf, J.; Leal, T.; Noel, S. Cystic fibrosis transmembrane conductance regulator modulators in cystic fibrosis: current perspectives. *Clin. Pharmacol. Adv. Appl.* **2016**, *8*, 127–140. (b) Lopes-Pacheco, M. CFTR modulators: shedding light on precision medicine for cystic fibrosis. *Front. Pharmacol.* **2016**, *7*, 1–20.

[4] http://www.genet.sickkids.on.ca/Home.html, last accessed on Nov 13, 2017.

[5] Amaral, M. D.; Farinha, C. M. Rescuing mutant CFTR: a multi-task approach to a better outcome in treating cystic fibrosis. *Curr. Pharm. Des.* **2013**, *19* (19), 3497–3508.

[6] (a) Moran, O. Model of the cAMP activation of chloride transport by CFTR channel and the mechanism of potentiators. *J. Theor. Biol.* **2010**, *262*, 73-79. (b) Li, C.; Ramjeesingh, M.; Wang, W.; Garami, E.; Hewryk, M.; Lee, D.; Rommens, J. M.; Galley, K.; Bear, C. E. ATPase activity of the cystic fibrosis transmembrane conductance regulator. *J. Biol. Chem.* **1996**, *271* (45), 28463–28468.

[7] (a) Hadida, S.; Van Goor, F.; Zhou, J.; Arumugam, V.; McCartney, J.; Hazlewood, A.; Decker, C.; Negulescu, P.; Grootenhuis, P.D. Discovery of N-(2,4-di-tert-butyl-5-hydroxyphenyl)-4-oxo-1,4-dihydroquinoline-3-carboxamide (VX-770, ivacaftor), a potent and orally bioavailable CFTR potentiator. *J. Med. Chem.* **2014**, *57*, 9776-9795. (b) Ramsey, B.W.; Davies, J.; McElvaney, N.G.; Tullis, E.; Bell, S.C.; Dřevínek, P.; Griese, M.; McKone, E.F.; Wainwright, C.E.; Konstan, M.W.; Moss, R.; Ratjen, F.; Sermet-Gaudelus, I.; Rowe, S.M.; Dong, Q.; Rodriguez, S.; Yen, K.; Ordoñez, C.; Elborn, J.S. A CFTR potentiator in patients with cystic fibrosis and the G551D mutation. *N Engl J Med*. **2011**, *365*, 1663-1672. (c) Van Goor, F.; Hadida, S.; Grootenhuis, P. D. J.; Burton, B.; Cao, D.; Neuberger, T.; Turnbull, A.; Singh, A.; Joubran, J.; Hazlewood, A.; Zhou, J.; McCartney, J.; Arumugam, V.; Decker, C.; Yang, J.; Young, C.; Olson, E. R.; Wine, J. J.; Frizzell, R. A.; Ashlock, M.; Negulescu, P. Rescue of CF airway epithelial cell function in vitro by a CFTR potentiator, VX-770. *Proc. Natl. Acad. Sci.* **2009**, *106* (44), 18825–18830.

[8] (a) De Boeck, K.; Munck, A.; Walker, S.; Faro, A.; Hiatt, P.; Gilmartin, G.; Higgins, M. Efficacy and safety of Ivacaftor in patients with cystic fibrosis and a non-G551D gating mutation. *J. Cyst. Fibros.* **2014**, *13* (6), 674–680. (b) Moss, R. B.; Flume, P. A.; Elborn, J. S.; Cooke, J.; Rowe, S. M.; McColley, S. A.; Rubenstein, R. C.; Higgins, M. Efficacy and safety of Ivacaftor in patients with cystic fibrosis who have an Arg117His-CFTR mutation: a double-blind, randomised controlled trial. *Lancet Respir. Med.* **2015**, *3* (7), 524–533.

[9] Van Goor, F.; Hadida, S.; Grootenhuis, P. D. J.; Burton, B.; Stack, J. H.; Straley, K. S.; Decker, C. J.; Miller, M.; McCartney, J.; Olson, E. R.; Wine, J. J.; Frizzell, R. A.; Ashlock, M.; Negulescu, P. A. Correction of the F508del-CFTR protein processing defect in vitro by the investigational drug VX-809. *Proc. Natl. Acad. Sci.* **2011**, *108*, 18843–18848.

[10] Wainwright, C.E.; Elborn, J.S.; Ramsey, B.W.; Marigowda, G.; Huang, X.; Cipolli, M.; Colombo, C.; Davies, J.C.; De Boeck, K.; Flume, P.A.; Konstan, M.W.; McColley, S.A.; McCoy, K.; McKone, E.F.; Munck, A.; Ratjen, F.; Rowe, S.M.; Waltz, D.; Boyle, M.P. Lumacaftor-Ivacaftor in patients with cystic fibrosis homozygous for Phe508del CFTR. *N. Engl. J. Med.* **2015**, *373*, 220-231.

[11] Galietta, L.J.V.; Luis, V.; Jayaraman, S.; Verkman, A.S. Cell-based assay for high-throughput quantitative screening of CFTR chloride transport agonists. *American Journal of Physiology*. **2001**, *281*,C1734-C1742.

[12] Yang, H.; Shelat, A A.; Guy, R.K.; Gopinath, V.S.; Ma, T.; Du, K.; Lukacs, G.L.; Taddei, A.; Folli, C.; Pedemonte, N.; Galietta, L. J.V.; Verkman, A.S. Nanomolar affinity small molecule correctors of defective ΔF508-CFTR chloride channel gating. *Journal of Biological Chemistry*, **2003**, *278*, 35079-35085.

[13] XlogP3 is a program for the prediction of the octanol/water partition coefficients of organic compounds. Renxiao, W.; Ying F.; Luhua L. A new atom-additive method for calculating partition coefficients, *J.Chem.Inf.Comput.Sci.* **1997**, *37*, 615-621.

[14] To obtain meaningful drug concentrations for the prediction of intrinsic clearance, non-specific binding is taking into account by correcting with the fraction unbound in microsomes (Fu,mic) or the fraction unbound in hepatocyte incubations (Fu,inc). (a) Obach, R.S. The importance of nonspecific binding in in vitro matrices, its impact on enzyme kinetic studies of drug metabolism reactions, and

implications for in vitro-in vivo correlations. *Drug. Metab. Dispos.*, **1996**, *24*, 1047-1049. (b) Gertz, M.; Kilford, P.J.; Houston, J.B.; Galetin, A. Drug lipophilicity and microsomal protein concentration as determinants in the prediction of the fraction unbound in microsomal incubations. *Drug. Metab. Dispos.*, **2008**, *36*, 535-542.

[15] Hwang, T.C.; Wang, F.; Yang, I.C.; Reenstra, W.W Genistein potentiates wild-type and delta F508-CFTR channel activity. *Am. J. Physiol.*, **1997**, *273*, C988-C998.

[16] Pedemonte, N.; Sonawane, N. D.; Taddei, A.; Hu, J.; Zegarra-moran, O.; Suen, Y. F.; Robins, L. I.; Dicus, C. W.; Willenbring, D.; Nantz, M. H.; Kurth, M. J.; Galietta, L. J. V; Verkman, A.S. Phenylglycine and sulfonamide correctors of defective DeltaF508 and G551D cystic fibrosis transmembrane conductance. *Mol. Pharmacol.* **2005**, *67* (5), 1797–1807.

[17] Van Goor, F.; Straley, K. S.; Cao, D.; Gonzalez, J.; Hadida, S.; Hazlewood, A.; Joubran, J.; Knapp, T.; Makings, L. R.; Miller, M.; Neuberger, T.; Olson, E.; Panchenko, V.; Rader, J.; Singh, A.; Stack, J. H.; Tung, R.; Grootenhuis, P. D.; Negulescu, P. Rescue of DF508-CFTR trafficking and gating in human cystic fibrosis airway primary cultures by small molecules. *Am J Physiol Lung Cell Mol Physiol* **2006**, *290* (6), 1117–1130.

[18] Frank, L.; Jack, B.; Christine, H. Escape from flatland: increasing saturation as an approach to improving clinical success. *J. Med. Chem.*, **2009**, *52*, 6752-6756.

[19] The TECC instrument is developed and sold by EP Design (Bertem, Belgium), and measures the potential difference (PD) and transmembrane resistance (R_t) over epithelial cells and these values are used to calculate the apparent short circuit current (I_{eq}) using Ohms law. The I_{eq} can be interpreted as the charge flow per time when the tissue is short circuited i.e. the transepithelial voltage V_t is clamped

to 0 mV and changes when ion channels in the apical or basolateral membrane of epithelial cells are opened or closed

[20] Yeh, H. I.; Sohma, Y.; Conrath, K.; Hwang, T. C. A common mechanism for CFTR potentiators. **2017**, 1–14.

[21] (a) Yu, H.; Burton, B.; Huang, C. J.; Worley, J.; Cao, D.; Johnson, J. P.; Urrutia, A.; Joubran, J.; Seepersaud, S.; Sussky, K.; Hoffman, B. J.; Van Goor, F. Ivacaftor potentiation of multiple CFTR channels with gating mutations. *J. Cyst. Fibros.* **2012**, *11* (3), 237–245. (b) Van Goor, F.; Yu, H.; Burton, B.; Hoffman, B. J. Effect of Ivacaftor on CFTR forms with missense mutations associated with defects in protein processing or function. *J. Cyst. Fibros.* **2014**, *13* (1), 29–36.

[22] (a) Wassvik, C.M.; Holmén, A.G.; Draheim, R.; Artursson, P.; Bergström, C.A.S. Molecular characteristics for solid-state limited solubility. *J. Med. Chem.* **2008**, *51*, 3035–3039.

[23] (a) Zhang, X.; Gong Z., Li J.; Lu, T. Intermolecular sulfur···oxygen Interactions: theoretical and statistical investigations. *J. Chem. Inf. Model.*, **2015**, *55*, 2138–2153. (b) Beno, B.; Yeung, K.; Bartberger, M.; Pennington, L.D.; Meanwell, N.A. A survey of the role of noncovalent sulfur Interactions in drug design. *J.Med.Chem.*, **2015**, *58*, 4383-4438

[24] Stella, V.J.; Borchardt, R.T.; Hageman, M.J.; Oliyai, R., Maag, H. Tilley, J.W. Prodrugs: Challenges and Rewards Part II. In *Biotechnology: Pharmaceutical Aspects*, 2007edition, Springer:New York, **2007**, 543-549.

[25] (a) Tam, F. W. K.; McAdoo, S. P. Fostamatinib disodium. *Drugs Future* **2011**, *36*, 273−280. (b) Kadow, J. F.; Ueda, Y.; Meanwell, N. A.; Connolly, T. P.; Wang, T.; Chen, C. P.; Yeung, K. S.; Zhu, J.; Bender, J. A.; Yang, Z.; Parker, D.; Lin, P. F.; Colonno, R. J.; Mathew, M.; Morgan, D.; Zheng, M.; Chien, C.; Grasela, D.

Inhibitors of human immunodeficiency virus type 1 (HIV-1) attachment 6. Preclinical and human pharmacokinetic profiling of BMS-663749, a phosphonooxymethyl prodrug of the HIV-1 attachment inhibitor 2-(4-benzoyl-1-piperazinyl)-1-(4,7-dimethoxy-1H-pyrrolo[2,3-c]pyridin-3-yl)-2-xoethanone (BMS-488043). *J. Med. Chem.* **2012**, *55*, 2048−2056.

[26] Dhareshwar, S.S.; Stella, V.J. Your prodrug releases formaldehyde: should you be concerned? No! *J. Pharm. Sci.* **2008**, *10*, 4184-4193.

[27] Wang, T.; Huang, X.-G. ; Liu, J.; Li, B.; Wu, J.-J. ; Chen, K.-X. ; Zhu, W.-L.; Xu, X.-Y.; Zeng, B.-B. An efficient one-pot synthesis of substituted 2-aminothiophenes via three-component Gewald reaction catalyzed by L-Proline. *Synlett*, **2010**, *9*, 1351-1354.

[28] Novosjolova, I. The Mukaiyama reagent: an efficient condensation agent. *Synlett* **2013**, *24*, 135-136.

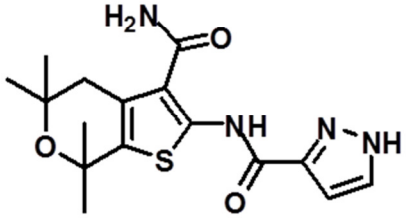
H2N
O
NH
N
NH
O
S
O

13

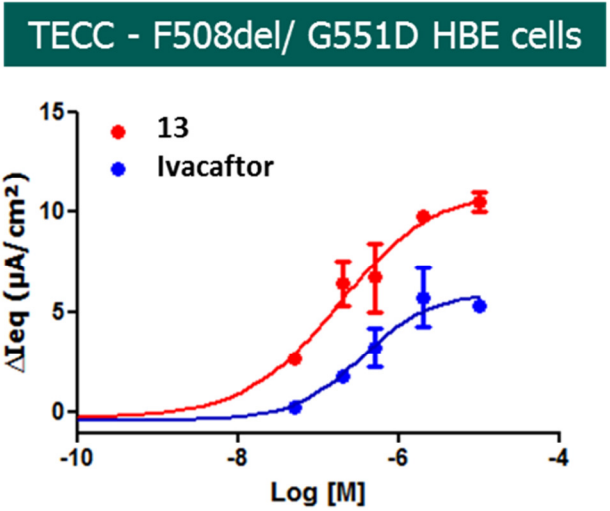
TECC - F508del/ G551D HBE cells
13
Ivacaftor
ΔIeq (μA/cm²)
15
10
5
0
-10
-8
-6
-4
Log [M]